# Direct patterning of noble metal nanostructures with a scanning tunneling microscope

F. Marchi, D. Tonneau,[a] H. Dallaporta, V. Safarov, and V. Bouchiat
*GPEC, UMR CNRS 6631, Université de la Méditerranée, Case 901, F-13288 Marseille, France*

P. Doppelt, R. Even, and L. Beitone
*ESPCI, F-75231 Paris, France*

(Received 19 November 1999; accepted 28 February 2000)

We demonstrate in this article the controlled deposition of noble metal dots and lines using local chemical vapor deposition in the tip–sample gap of a scanning tunneling microscope. 3 nm diam rhodium dots have been patterned by local decomposition of an inorganic precursor, which was synthesized on purpose. Deposition is obtained on gold surfaces by applying a series of negative voltage pulses on the sample exceeding a voltage threshold of around 2 V. The influence of kinetics parameters (pulse voltage duration and number, as well as the effect of gas pressure) are presented. In a second step, the deposition process has been applied on hydrogenated silicon (100) surfaces. These samples were previously hydrogen passivated using two different wet etching operations, leading surface dangling bonds saturated by either mono- or di-hydride bonds. The difference in the deposition processes observed in both cases is discussed. © *2000 American Vacuum Society.*
[S0734-211X(00)06903-1]

## I. INTRODUCTION

The high resolution reached by scanning probe microscopes (SPMs) i.e., atomic force microscopy (AFM) or scanning tunneling microscopy (STM) suggested that these techniques could be particularly suitable for lithography applications at scales not reachable by lithography techniques commonly used in microelectronics industry [i.e., ultraviolet or electron beam lithography]. Processes for lithography at the nanometer scale based on SPM techniques[1–3] are now widely investigated in two different ways: either for mask generation or direct patterning.

For example, an oxide mask can be drawn on hydrogenated silicon by voltage-enhanced oxidation.[4–6] This mask can lead to silicon nanowires after a silicon wet etching.[6]

In the case of direct writing, the step of mask transfer is not necessary because the final pattern is directly fabricated by the SPMs. Among these mask-less techniques,[7–11] those that seem to offer the best resolution (without a mandatory ultrahigh vacuum facility), are the STM assisted chemical vapor deposition (STM-CVD) techniques.[8–11] They are based on the local decomposition of a gaseous molecular precursor in the tunnel gap of a highly biased STM. Several groups have implemented this technique, mainly using organometallic precursors and a silicon surface. In particular metallic nanostructures with a 10 nm linewidth can be realized in a reproducible way.[8]

A novel interest in these techniques emerged ones the last few years because they can help in elaborating single electron devices. Indeed the core of these devices can be made of nanometer-sized metallic dots, each dot being connected between each other by small capacitance tunnel junctions. These devices, based on the Coulomb blockade effect,[12,13] require a lithography resolution as high as several nanometers to reach room temperature operation.[14] Such a resolution remains out of range for state-of-the-art conventional lithography techniques.

Since devices robust against atmosphere and humidity aggression are envisioned, we focus on a direct writing process of noble metal dots. For that purpose, precursors of several different noble metals (Au, Rh, Ir) have been synthesized. However, we found that the rhodium-based precursor has the best stability and leads to more reproducible results. Therefore, the extensive study was performed on that material. As a first step, the influence of duration, number and amplitude of voltage pulses, as well as the effect of gas pressure on the deposition rate have been studied on gold surfaces. Finally, the process has been transferred on hydrogenated silicon (100) samples, opening the way to the realization of a connected device.

## II. EXPERIMENT

The principle of the STM assisted CVD technique is shown on Fig. 1. Gaseous molecules present in the gap between the tip and surface are decomposed by application of a series of voltage pulses.[8] The feedback loop of the STM is maintained during the whole deposition process. However, the pulse width $T_p$ has to be chosen shorter than the time constant of the STM feedback loop, while the dead time $T_r$ between pulses has to be longer than this time constant. This allows the tip altitude to remain constant during deposition, while the tip has time to retract between two pulses. Such a procedure prevents any contact between the tip and deposit during its growth (assuming that the other parameters are chosen such that the tunnel gap is not completely filled during one pulse).

In our experimental setup the STM time constant was ~1

[a]Author to whom correspondence should be addressed; electronic mail: tonneau@gpec.univ-mrs.fr

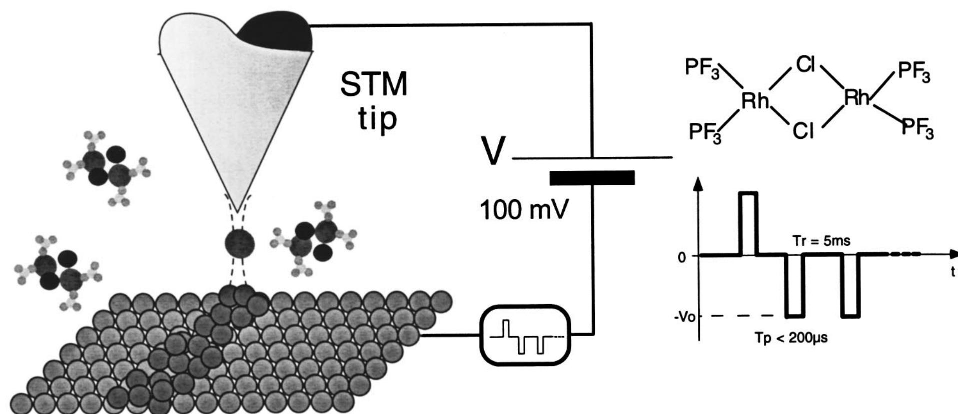


FIG. 1. (Left) Schematics of the STM assisted CVD technique. (Top right) detailed formula of the rhodium precursor used for the extensive study (Bottom right) time trace of the pulses applied on the sample for dot deposition.

ms and in all experiments the repetition rate was fixed at 200 Hz.

The STM is placed inside a pumped stainless steel chemical reactor, with base pressure of $5\times10^{-7}$ mbar before precursor introduction. This reactor is fixed on a bulk steel plate insulated from low frequency vibrations by shock springs. Inside the reactor chamber, the STM itself is fixed on a Viton stack, consisting of a series of metallic plates insulated from each other by Viton rings in order to damp vibrations in the range of kHz. More details can be found in Ref. 15.

The gold, iridium and rhodium precursors were the molecules $(PF_3)AuCl$.[16] Ir(hfac)1, 5-COD,[17] and $[(PF_3)_2RhCl]_2$[18,19] (see Fig. 1 right, for a detailed formula of this latter precursor). All of them have been synthesized for CVD purposes.[18,19] Inorganic molecules are preferred over organic ones in order to avoid carbon contamination on surfaces. These precursors are solid at room temperature and stored in a small chamber connected to the reactor via an inlet pipe closed by a needle valve.

Experiments are performed in a static atmosphere of pure precursor due to crystal sublimation. The gas pressure was varied in the range of $10^{-4}-10^{-2}$ mbar by opening the connecting valve. Gaseous molecules in the gap between tip and sample are decomposed by application of a series of voltage pulses of width in the range 20–200 $\mu$s and amplitude between 2 and 3 V.

The first series of experiments has been performed on gold-coated mica substrates. These gold samples are *e*-gun evaporated under high vacuum at high temperature (400 °C). They show atomically flat Au (111) terraces as large as about $100\times100\,\mathrm{nm}^2$.[20] These flat terraces provide a surface free from nanometer-sized artifacts, thus suitable for testing our CVD process. The precursors were evaluated and compared considering their stability at room temperature and the reliability of the deposition process. The best results were obtained with the rhodium-based precursor. So an extensive study of deposition kinetics was performed on that material.

In a second step, the deposition process has been transferred on low-doped hydrogenated silicon (100) substrates ($\rho=5-10\,\Omega$ cm) which provide a surface suitable for low temperature characterization of connected devices.

STM tips are prepared by electrochemical etching[21] of a platinum wire. This technique leads to very sharp and symmetric STM tips. Typical tips have a 5–10 nm diam apex and do not lead to image artifacts due to multiple tip effects.

STM imaging is performed using constant-current feedback. Typically, gold surfaces are imaged with a sample bias of 100 mV, whereas silicon surfaces are observed under 1.5 V. In both cases, the tunnel current flow is set to 300 pA. During lithography, an $XY$ STM scan is stopped while a series of pulses is superimposed on the constant bias. The obtained pattern is imaged with the same parameters just after deposition.

## III. RESULTS AND DISCUSSION

### A. Deposition on gold surfaces

Figure 2 presents typical STM images of patterned rhodium deposits. In order to check the reliability of our precursors, we first performed high voltage and high speed lithography using a similar procedure as presented in Ref. 11. A typical result of a 20 nm-wide line drawn at 10 V is presented in Fig. 2 (top left). However, the pulse method presented in Sec. II shows that a much better resolution can be achieved (top and bottom right). Dots of controlled relative position, size (as small as 3 nm diameter), and geometry are obtained. First of all, it was found that noticeable dot deposition is only obtained when the sample bias is higher than a threshold of $|-1.9|$ V. For positive pulse voltages, even at amplitudes as high as 6 V, no deposition was observed on the substrate. This suggest that local heating is not the only mechanism involved. Furthermore, the metallic compound experiences a reduction during the process and is thus deposited on the cathode (i.e., the negatively biased electrode). Our results differ from experiments of another group[8] performed under other experimental conditions for which deposits occurred for both polarities.

Due to the tiny volume of the deposited dots, their composition cannot be directly analyzed. However, the STM tip has been analyzed by local x-ray photoelectron spectroscopy after a series of reverse polarity experiments. Those are performed by applying positive voltage pulses on the gold sample (that means under conditions for which deposition does not occur on the substrate but on the tip). This tip analy-

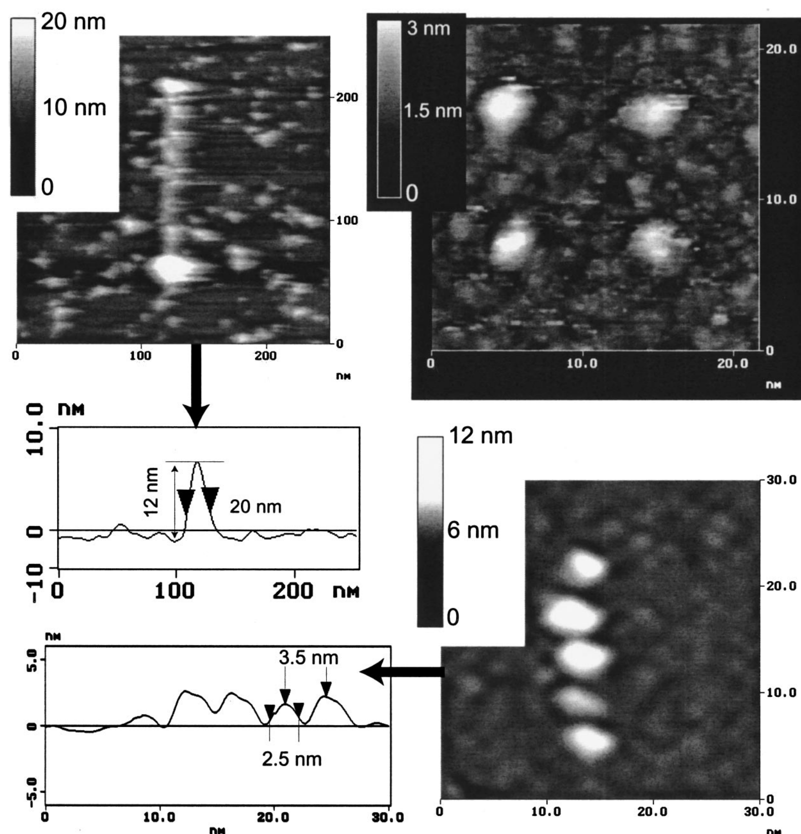


FIG. 2. STM pictures and cross sections of the deposited rhodium nanostructures. (Top left) Example of a 20-nm-wide line drawn using high-speed (250 $nm\,s^{-1}$) 400 scans with a $-6$ V continuous sample bias. (Top and bottom right) Rhodium dots deposited on gold using the pulse technique described in the text. Top deposits were obtained applying a single—150 ms—long pulse at $-2.9$ V, whereas each dot in the bottom right picture was obtained using a series of 100 pulses of 50 $\mu$s at $-2.8$ V.

sis has evidenced the presence of rhodium and traces of chlorine. Neither phosphorus nor fluorine have been detected. These results are similar to those obtained in classical CVD processes.[18] It can be assumed that the dot composition on the gold surface is of the same nature as deposits on the tip.

Using the other precursors presented above, gold dots and iridium dots have been deposited under similar experimental conditions. In all cases, deposits are observed only for negative sample bias pulses exceeding a threshold depending on the precursor (see Table I). Note that these thresholds follow the same stability hierarchy as observed in conventional CVD furnaces (Table I).

The saturation pressure of the iridium precursor at room temperature (about $10^{-3}$ mbar) is about ten times lower than the other precursors. Such a low value influences drastically both deposition rate and experiment reliability (see Sec. III B). The gold precursor is very unstable and the gas pressure decreases in the reactor with a time constant of about 15 min, too short to perform reproducible experiments.

Consequently, the rhodium precursor has been chosen for potential applications and we will finally focus on that material.

TABLE I. CVD characteristics of the three tested noble metal precursors.

| Precursor | Voltage threshold (V) | Deposition rate under pulse voltage of $-2.8$ V ($nm^3\,s^{-1}$) | Temperature decomposition threshold in a CVD furnace (°C) |
|---|---|---|---|
| $[RhCl(PF_3)_2]_2$ | $-1.9$ | 650 | 150 [a] |
| $AuCl(PF_3)$ | $-2.5$ | 130 | 150 [b] |
| Ir(hfac)1,5-COD | $-2.7$ | 30 | 230 [c] |

[a]See Ref. 18.
[b]See Ref. 16.
[c]See Ref. 17.

## B. Kinetics of the rhodium deposition process

We have measured the deposited volume dependence of the deposit as a function of the number of pulses, their duration and amplitude. On the other hand the influence of gas pressure has been investigated.

The inset of Fig. 3 shows the measured deposit volume as a function of the number of pulses for increasing pulse widths. The deposited volume varies linearly with the pulse number. Moreover, the slopes of the fitted line increase with the pulse width. Thus one has to consider the integrated exposure dose which can be simply defined as the product between the pulse number and pulse width. Figure 3 shows the variation of the deposited volume with the exposure dose for a pulse width, of 200, 100, and 50 $\mu$s, respectively. For a given dose and for pulse width longer than 100 $\mu$s, the dot volume does not depend on the pulse width. For pulses shorter than 100 $\mu$s, we observe a strong deviation from this dose dependence. The slope is smaller and the size fluctuations are very high at low exposures. In many cases, the first traces of deposit appear only after a total exposure time of $\sim$30 ms, i.e., the first several hundred pulses produced no deposit at all. For a pulse width below 20 $\mu$s, no deposit was observed, even for a large number of pulses.

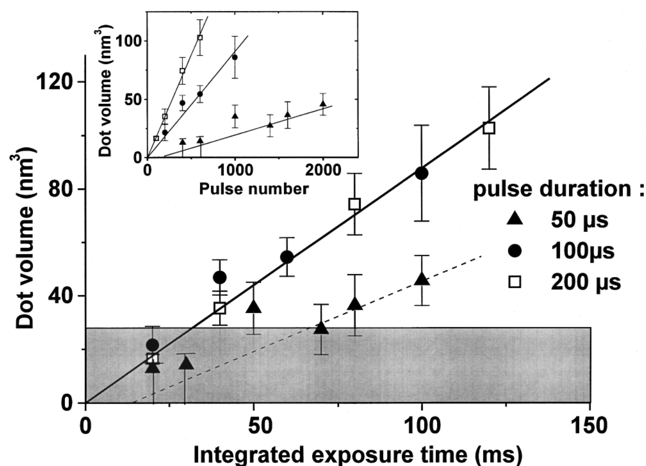


FIG. 3. Dependence of the rhodium dot volume on the integrated exposure time for three pulse widths: 50, 100, and 200 $\mu$s. (Inset) same data plotted as a function of the pulse number. The gas pressure is $10^{-2}$ mbar and the pulse amplitude is $-2.8$ V.

The effect of gas pressure on deposition rate has been investigated with a pulse amplitude of $-2.8$ V and duration of 200 $\mu$s (Fig. 4). The deposition rate is proportional to the gas pressure in the range of $10^{-3}-10^{-2}$ mbar. No deposition was observed for pressure below $10^{-3}$ mbar.

The linear relationship between the deposition rate and the gas pressure suggests that the reaction is mass-transport limited. The reaction can occur either in the layer adsorbed on the surface or in the gas phase in the tip–sample gap.

Assuming that the molecule transport is governed by the gas phase, the molecule flux per unit time and surface is given by the kinetics theory of gases:

$$\Phi(m^{-2}s^{-1}) = -\frac{P}{\sqrt{2\pi m k_B T}}, \quad (1)$$

where $P$, $m$ and $T$ are the gas pressure, molecule mass and gas temperature, respectively, and $k_B$ is Boltzman's constant.

The molecules are decomposed in a CVD active volume between the tip and the sample. One can reasonably assume that this volume consists of a cylinder with base on the order of the tip apex radius ~5 nm (it also corresponds to the typical deposit size of 3 nm) and the height of the order of the tip–surface distance ~0.5 nm.

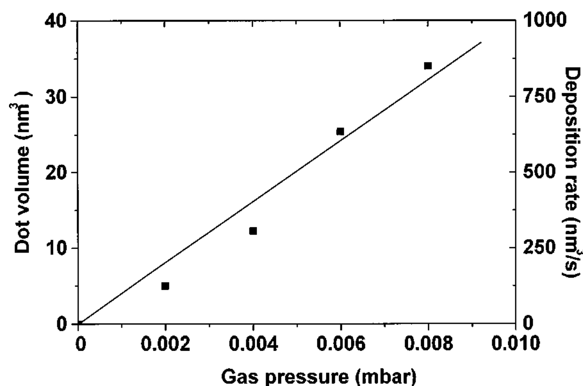


FIG. 4. Dependence of the deposition rate on gas pressure. The pulse width $T_p$ and amplitude are, respectively, 200 $\mu$s and $-2.8$ V.

However, due to the tightness of the tip–sample distance regarding the curvature radius of the STM tip, it induces a screening effect limiting the molecule flux in the CVD-active cylinder just below the tip apex.[15] This shadow decreases the molecule flux given by Eq. (1) by at least a factor of 2. Finally, with a gas pressure of $10^{-2}$ mbar, the flux in the active region is expected to be around $\Phi = 3000$ molecule nm$^{-2}$ s$^{-1}$.

The maximum deposition rate is obtained from the assumption that all molecules impinging on the surface of the active volume are decomposed. Since the precursor molecule contains two rhodium atoms, the rhodium atom flux is expected to be twice the molecule flux, i.e., 6000 nm$^{-2}$ s$^{-1}$ for a gas pressure of $10^{-2}$ mbar. Assuming that deposits are composed of pure rhodium (density 12.4 g/cm$^3$) and taking into account the atomic weight of Rh (102.9 g), a deposition rate of 800 nm$^3$/s of exposure is expected, assuming that the CVD efficiency is 100%. This rather rough evaluation is in quite good agreement with experimental results presented in Fig. 4. So we can conclude that for long pulses and at relatively high pressure, the reaction is mass-transport limited and its efficiency is very high (close to 1).

It is interesting to evaluate how many molecules enter the active region during one pulse. For typical conditions of gas pressure of $10^{-2}$ mbar and a pulse duration of 200 $\mu$s, only a few molecules (~6) cross the active region during one pulse. Under these conditions, we observe the linear dependence of the deposition rate on the exposure and on the gas pressure.

However, for the pressure of $10^{-3}$ mbar and the pulse duration of 200 $\mu$s the mean number of molecules present in the active region during one pulse is only ~0.6. The fact that the presence probability of molecules during the pulse becomes lower than unity for short pulses and low gas pressures could explain why deposition kinetics are essentially modified under these conditions.

Indeed, it could seem that the low presence probability of a molecule during pulse application might be compensated by a higher number of pulses: for the same exposure, one should observe the same deposit volume. However as it is seen from Fig. 3, this is not observed. We attribute this effect to a problem of nucleation. During to the rather long time between two pulses (5 ms), atoms can diffuse on the surface. Therefore the deposition seems to be delayed due to the nonstability of too small rhodium clusters. Consequently, the formation of a stable cluster requires a minimal number of molecules to be decomposed during the same pulse. The probability $P(k)$ that $k$ molecules cross the active region during the same pulse for a mean molecule number $n$ per pulse is given by the Poisson distribution: $P(k) = (n^k/k!)e^{-n}$.
For a mean molecule number per pulse $n=6$, the probability of $\Sigma_{k\geqslant 4}P(k)$ having more than four molecules during one pulse is 94%, whereas for $n=0.6$, this quantity shrinks to 0.3%. This could explain why, in the short pulse regime, one

has to apply hundreds of pulses before the formation of the first stable cluster, which permits the subsequent growth of the deposit. It possibly also explains the broad size dispersion of dot sizes deposited at low doses.

### C. Deposition on hydrogenated silicon surfaces

STM experiments require us to work on conductive substrates. Consequently, the native oxide layer has to be removed from the silicon surface. Silicon samples are prepared by two different wet etching processes: $T_1$ and $T_2$, which are known to passivate the surfaces by hydrogen atoms,[22] which impede surface oxidation during air exposure. These treatments consist of a first step of surface degreasing followed by a series of oxidation and stripping. The difference between treatments $T_1$ and $T_2$ remains in the final step, which is either a dip etching in HF 5% during 30 s ($T_1$), or substrate immersion in BHF ($NH_4F$/HF 7:1 vol.) followed by immersion in $NH_4F(T_2)$.

First, experiments were performed on these passivated surfaces using conditions similar to gold samples. No deposits were observed on silicon for both kinds of treated samples and for both pulse polarities. We attribute this to the fact that rhodium nucleation seems impossible directly on hydrogen passivated surfaces, which are known to be nonreactive surfaces.

In order to perform lithography, a new biasing procedure has been implemented. It involves pulses of different polarities applied in the same series. For $T1$-treated samples, rhodium dots have been deposited provided that positive voltage pulses higher than +6 V were applied on the substrate prior to the application of negative pulses. However, it remained impossible to obtain deposit on surfaces prepared by treatment $T_2$ under the same conditions.

Studies on oxide mask pattern generation on hydrogenated silicon surfaces have shown that hydrogen can be locally removed from silicon surfaces by an AFM tip by application of a positive bias on the sample.[3] In our case, the positive voltage pulses previously applied to the silicon sample induce a local hydrogen desorption, which locally enhances the rhodium nucleation step and finally allows rhodium dot deposition. The value of pulse voltage necessary to remove hydrogen from the passivated silicon surface is consistent with results found in the literature.[23]

Figure 5 shows a three-dimensional (3D) AFM image of a typical rhodium dot deposited on a (100) silicon surface. Local depassivation of the silicon surface was obtained by application of ten voltage pulses at 6 V followed by a series of 200 negative voltage pulses at −2.9 V. For both polarities, the pulse duration was 200 $\mu$s. The resulting dot size is about 3 nm wide and 2 nm high. One can also notice that the silicon surface is much rougher (rms=1 nm) than the gold surface previously presented.

When substrates are prepared using treatment $T_2$, dot deposition still remains impossible. In fact, dip etching in HF solution leads to passivation of the silicon surface by mono- and dihydride bonds.[24] Thermal desorption spectroscopy measurements have shown that the temperature desorption of

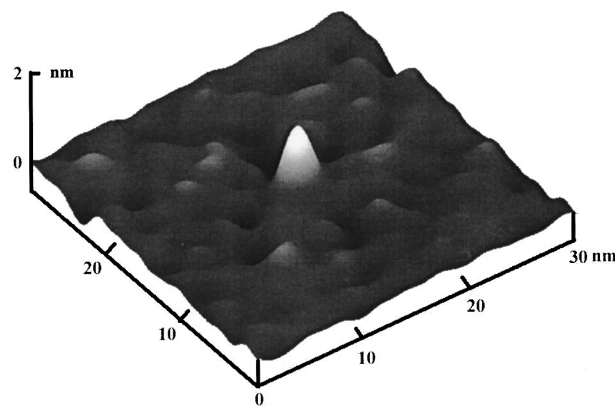


FIG. 5. 3D AFM image of a rhodium dot deposited on a (100) silicon substrate prepared using process $T1$. The gas pressure was 1.5 $\times 10^{-2}$ mbar. The dot was obtained after a series of ten pulses of 200 $\mu$s duration at sample bias +6 V followed by 200 pulses of 200 $\mu$s at sample bias −2.9 V.

hydrogen from the silicon surface depends on the nature of the chemical bonds and is 410 and 530 °C, respectively, for di- and monohydride bonds, respectively. The dihydride bonds can be locally removed by application of positive voltage pulses to the sample and consequently the surface is locally depassivated, which allows rhodium nucleation and growth. However, treatment $T_2$ induces a stronger surface passivation by monohydride bonds, which still impedes local surface depassivation under the STM tip even for a pulse amplitude as high as 8 V.

### D. Process resolution

It has been demonstrated that nanometer-sized metallic dots with an aspect ratio around 1 and sometime exceeding 1 can be deposited by the STM assisted CVD technique in a reproducible way on gold and silicon surfaces. The control of their size and position is suitable for elaboration of room temperature single electron devices. However, the most important parameter for that purpose is the relative distance between dots, as it defines the tunnel barrier in such devices. It has to be in the range of 1 nm for keeping a reasonable conductance. Furthermore it must be geometrically well controlled as the tunnel coupling between dots exponentially depends on it. Figure 2 (bottom right) shows an example of a series of rhodium dots drawn very close to each other. The distance between dots seems to be controlled by the tip radius. We would like to fabricate a similar structure aligned with respect to electrical contacts deposited on the surface.

## IV. CONCLUSION

Few nanometer wide rhodium dots can be deposited on gold surfaces by local decomposition of $[(PF_3)_2RhCl]_2$ molecules under a STM tip during application of voltage pulses to the substrate. The reaction occurs when negative pulses are applied to the substrate surface above a threshold of $|-1.9|$ V. The deposition rate increases with pulse amplitude and is mass transport limited under low gas pressure. Under these conditions, the reaction efficiency reaches 100%.

Under the same conditions, rhodium dots cannot be deposited on hydrogenated silicon surfaces since hydrogen atom's presence on the surface inhibits dot nucleation. However, hydrogen can be locally removed from the substrate surface when positive voltage pulses are applied to the sample. Then, application of negative pulses to the sample leads again to rhodium nucleation and dot deposition.

## ACKNOWLEDGMENTS

This study is supported by CEC ESPRIT Project No. 23214 entitled 'FASEM' (Fabrication and Architecture of Single Electron Memories). The authors wish to thank F. Thibaudau for fruitful discussions.

[1]For a review on early developments in STM lithography, see R. Wiesendanger, Appl. Surf. Sci. **54**, 271 (1992).
[2]V. Bouchiat and D. Esteve, Appl. Phys. Lett. **69**, 3098 (1996) and references therein.
[3]J. A. Dagata, J. Schneir, H. H. Harary, C. J. Evans, M. T. Postek, and J. Bennett, Appl. Phys. Lett. **56**, 2001 (1990).
[4]E. S. Snow and P. M. Campbell, Appl. Phys. Lett. **64**, 1932 (1994).
[5]F. Marchi, V. Bouchiat, H. Dallaporta, V. Safarov, D. Tonneau, and P. Doppelt, J. Vac. Sci. Technol. B **16**, 2952 (1998); R. Garcia, M. Calleja, and F. Perez-Murano, Appl. Phys. Lett. **72**, 2295 (1998).
[6]P. M. Campbell, E. S. Snow, and P. J. McMarr, Appl. Phys. Lett. **66**, 1388 (1995).
[7]D. P. Adams, T. M. Mayer, and B. S. Scwartentruber, Appl. Phys. Lett. **68**, 2210 (1996).
[8]E. E. Ehrichs, S. Yoon, and A. L. de Lozanne, Appl. Phys. Lett. **53**, 2287 (1988); E. E. Ehrichs, W. F. Smith, and A. L. de Lozanne, J. Vac. Sci. Technol. B **9**, 1380 (1991).
[9]S.-T. Yau, D. Saltz, and M. H. Nayfeh, J. Vac. Sci. Technol. B **9**, 1371 (1991).
[10]F. Thibaudau, J. R. Roche, and F. Salvan, Appl. Phys. Lett. **64**, 523 (1994).
[11]S. Rubel, X.-D. Wang, and A. L. de Lozanne, J. Vac. Sci. Technol. B **13**, 1332 (1995).
[12]D. D. Averin and K. K. Likharev in *Mesoscopic Phenomena in Solids*, edited by B. Altshuler *et al.* (Elsevier, Amsterdam, 1991).
[13]*Single Charge Tunneling*, edited by H. Grabert and M. H. Devoret (Plenum, New York, 1992).
[14]J. Shirakashi, K. Matsumoto, N. Miura, and M. Konagai, Appl. Phys. Lett. **72**, 1893 (1998).
[15]F. Marchi, D. Tonneau, R. Pierrisnard, V. Bouchiat, V. Safarov, H. Dallaporta, P. Doppelt, and R. Even, J. Phys. IV **9**, 733 (1999).
[16]W. Fuss and M. Rühe, Z. Naturforsch. **47b**, 591 (1992).
[17]C. Xu and T. H. Baum, Chem. Mater. **10**, 2329 (1998).
[18]P. Doppelt, V. Weigel, and P. Guinot, Mater. Sci. Eng., B **17**, 143 (1993).
[19]P. Doppelt, L. Ricard, and V. Weigel, Inorg. Chem. **32**, 1039 (1993).
[20]H. Klein, C. Fauquet, W. Blanc, R. Pierrisnard, V. Bouchiat, Ph. Dumas, and F. Salvan, Proceedings of STM'99, Seoul, 1999, Korea, p. 184 (unpublished).
[21]L. Libioulle, Y. Houbion, and J. M. Gilles, Rev. Sci. Instrum. **66**, 97 (1995).
[22]R. A. Venkatesware, F. Ozanam, and J.-N. Chazalviel, J. Electrochem. Soc. **138**, 153 (1991).
[23]T. C. Chen, C. Wang, G. C. Abeln, J. R. Tucker, J. W. Lyding, P. Avouris, and R. E. Walkup, Science **268**, 1590 (1995).
[24]T. Tagahagi, I. Nagai, A. Ishitani, H. Kuroda, and Y. Nagasawa, J. Appl. Phys. **64**, 3516 (1988).